Inorg. Chem. **2006**, *45*, 8838–8840

Inorganic Chemistry

Communication

Triggered Ligand Release Coupled to Framework Rearrangement: Generating Crystalline Porous Coordination Materials

Junhua Jia, Xiang Lin, Alexander J. Blake, Neil R. Champness,* Peter Hubberstey,* Limin Shao, Gavin Walker, Claire Wilson, and Martin Schröder*

School of Chemistry and School of Mechanical, Materials & Manufacturing Engineering, University of Nottingham, University Park, Nottingham NG7 2RD, U.K.

Received June 18, 2006

A robust 3-D porous structure of formula $[Ln_2(PDC)_3(DMF)_2]_\infty$ has been constructed from lanthanide cations (Ln = Er^{3+} or Y^{3+}) and the non-linear anionic bridging ligand, pyridine-3,5-dicarboxylate (PDC^{2-}) in dimethylformamide (DMF). The solvated framework polymers $\{[M_2(PDC)_3(DMF)_2]\cdot n(solv)\}_\infty$ (M = Er, Y) undergo a solid-state, crystal-to-crystal reaction upon heating and are converted via loss of both sorbed and coordinated solvent and rearrangement of the framework core to give a desolvated and porous form with retention of structural integrity. This structural transfer is the first crystallographically characterized system with lanthanide metal ions. These porous products are shown to be effective absorbants for H_2, N_2, and benzene.

Metal–organic coordination polymers have attracted much attention owing to the possibility of using flexible design methodologies to construct porous frameworks with channels of targeted size and shape.[1] Such materials have enormous potential applications for molecular storage and separation, catalysis, and ion exchange.[2,3] We have recently reported a range of highly unusual framework materials of previously unreported topologies based upon lanthanide centers with *N*-oxide heterocyclic ligands.[4] We were especially interested in controlling the stereochemistry and connectivity at the metal centers, as well as the degree of aggregation[5] and topology in these and related lanthanide materials. We report herein the crystal-to-crystal solid-state conversion of materials derived from lanthanide(III) cations and pyridine-3,5-dicarboxylate anions (PDC^{2-}). The PDC^{2-} dianion was chosen for its non-linear rigidity, which reduces the potential for interpenetration,[6] and its negative charge, which obviates the need to find space for non-coordinated anions within the lattice of the resultant framework, thereby providing more solvent-accessible space within the bulk material. In addition, we argued that the high formal 3+ charge on the lanthanide ion has the potential to enhance possible interactions between the Lewis acid metal and adsorbed species within the resultant porous framework material.

We find that the solvated products, $\{[M_2(PDC)_3(DMF)_2]\cdot n(solv)\}_\infty$ (M = Er, Y), undergo a solid-state, crystal-to-crystal transformation upon heating to afford, *via* loss of both sorbed and coordinated solvent and rearrangement of the mode of binding of the carboxylate donors, the desolvated, porous form $\{[M_2(PDC)_3]\}_\infty$ (M = Er, Y) with retention of

---

* To whom correspondence should be addressed. E-mail: neil.champness@nottingham.ac.uk (N.R.C.), peter.hubberstey@nottingham.ac.uk (P.H.), m.schroder@nottingham.ac.uk (M.S.). Fax: +44 115 9513563.

(1) Blake, A. J.; Brooks, N. R.; Champness, N. R.; Hanton, L. R.; Hubberstey, P.; Schröder, M. *Pure Appl. Chem.* **1998**, *70*, 2351–2357. Champness, N. R.; Schröder, M. *Curr. Opin. Solid State Mater. Chem.* **1998**, *3*, 419–424. Eddaoudi, M.; Moler, D. B.; Li, H.; Chen, B.; Reineke, T. M.; O'Keeffe, M.; Yaghi, O. M. *Acc. Chem. Res.* **2001**, *34*, 319–330. Evans, O. R.; Lin, W. *Acc. Chem. Res.* **2002**, *35*, 511–522.

(2) Blake, A. J.; Champness, N. R.; Hubberstey, P.; Li, W.-S.; Withersby, M. A.; Schröder, M. *Coord. Chem. Rev.* **1999**, *183*, 117–138. James, S. L. *Chem. Soc. Rev.* **2003**, *32*, 276–288. Janiak, C. *Dalton Trans.* **2003**, 2781–2804. Kitagawa, S.; Kitaura, R.; Noro, S. D. *Angew. Chem., Int. Ed.* **2004**, *43*, 2334–2375. Kitaura, R.; Iwahori, F.; Matsuda, R.; Kitagawa, S.; Kubota, Y.; Takata, M.; Kobayashi, T. C. *Inorg. Chem.* **2004**, *43*, 6522–6524.

(3) Blake, A. J.; Champness, N. R.; Khlobystov, A. N.; Parsons, S.; Schröder, M. *Angew. Chem., Int. Ed.* **2000**, *39*, 2317–2320. Cussen, E. J.; Claridge, J. B.; Rosseinsky, M. J.; Kepert, C. J. *J. Am. Chem. Soc.* **2002**, *124*, 9574–9581. Khlobystov, A. N.; Brett, M. T.; Blake, A. J.; Champness, N. R.; Gill, P. M. W.; O'Neill, D. P.; Teat, S. J.; Wilson, C.; Schröder, M. *J. Am. Chem. Soc.* **2003**, *125*, 6753–6761. Uemura, T.; Kitagawa, S. *J. Am. Chem. Soc.* **2003**, *125*, 7814–7815. Zhao, X.; Xiao, B.; Fletcher, A. J.; Thomas, K. M.; Bradshaw, D.; Rosseinsky, M. J. *Science* **2004**, *306*, 1012–1015. Fletcher, A. J.; Cussen, E. J.; Bradshaw, D.; Rosseinsky, M. J.; Thomas, K. M. *J. Am. Chem.* Soc. **2004**, *126*, 9750–9759. Yamada, K.; Yagishita, S.; Tanaka, H.; Tohyama, K.; Adachi, K.; Kaizaki, S.; Kumagai, H.; Inoue, K.; Kitaura, R.; Chang, H.-C.; Kitagawa, S.; Kawata, S. *Chem.—Eur. J.* **2004**, *10*, 2647–2660. Maji, T. K.; Uemura, K.; Chang, H.-C.; Matsuda, R.; Kitagawa, S. *Angew. Chem., Int. Ed.* **2004**, *43*, 3269–3272. Panella, B.; Hirscher, M. *Adv. Mater.* **2005**, *17*, 538–541. Kubota, Y.; Takata, M.; Matsuda, R.; Kitaura, R.; Kitagawa, S.; Kato, K.; Sakata, M.; Kobayashi, T. C. *Angew. Chem., Int. Ed.* **2005**, *44*, 920–923.

(4) Long, D.-L.; Blake, A. J.; Champness, N. R.; Wilson, C.; Schröder, M. *J. Am. Chem. Soc.* **2001**, *123*, 3401–3402. Long, D.-L.; Blake, A. J.; Champness, N. R.; Wilson, C.; Schröder, M. *Angew. Chem., Int. Ed.* **2001**, *40*, 2444–2447. Long, D.-L.; Blake, A. J.; Champness, N. R.; Wilson, C.; Schröder, M. *Chem.—Eur. J.* **2002**, *8*, 2026–2033. Long, D.-L.; Hill, R. J.; Blake, A. J.; Champness, N. R.; Hubberstey, P.; Proserpio, D. M.; Wilson, C.; Schröder, M. *Angew. Chem., Int. Ed.* **2004**, *43*, 1851–1854. Hill, R. J.; Long, D.-L.; Champness, N. R.; Hubberstey, P.; Schröder, M. *Acc. Chem. Res.* **2005**, *38*, 335–348.

(5) Doble, D. M. J.; Benison, C. H.; Blake, A. J.; Fenske, D.; Jackson, M. S.; Kay, R. D.; Li, W.-S.; Schröder, M. *Angew. Chem., Int. Ed.* **1999**, *38*, 1915–1918.

(6) Withersby, M. A.; Blake, A. J.; Champness, N. R.; Cooke, P. A.; Hubberstey, P.; Schröder, M. *New J. Chem.* **1999**, *23*, 573–575 and references cited therein.

10.1021/ic061095u CCC: $33.50

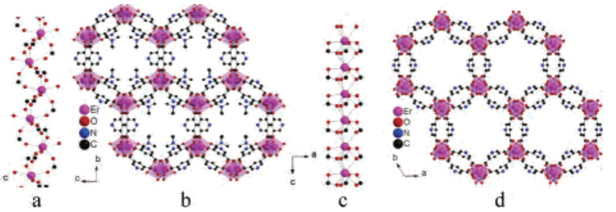

Figure 1. Views of the structure of **1**: (a) zigzag connection between adjacent Er^{3+} centers; (b) channels with a view along the orthorhombic *a* axis showing coordinated DMF molecules protruding into the channel space. Views of the structure of **3**: (c) the shorter linear connection between adjacent Er^{3+} centers; (d) view of the open channels along the hexagonal *c* axis after removal of coordinated DMF molecules.

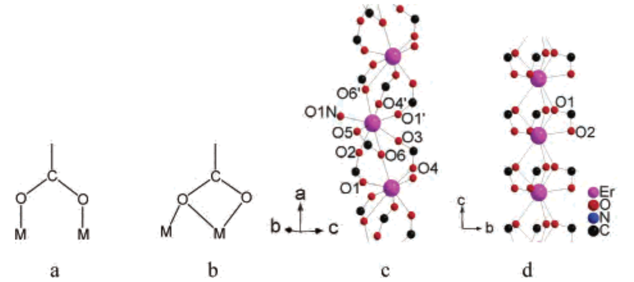

Figure 2. (a and b) Connection modes between each M^{3+} center and carboxylate anions. (c and d) Coordination around the M^{3+} centers in **1** and **3**, respectively. O1N (see part c) represents the O donor from coordinated DMF, removed during the synthesis of **3**.

crystallinity, structural integrity, and metal−PDC^{2-} coordination. These represent rare examples[7] and the first crystallographically characterized system with lanthanide metal ions[8] of metal−organic frameworks that retain crystalline structural integrity upon removal of coordinated solvent and framework rearrangement.

The isomorphous compounds $\{[Er_2(PDC)_3(DMF)_2]\cdot n(solv)\}_\infty$ (**1**) and $\{[Y_2(PDC)_3(DMF)_2]\cdot n(solv)\}_\infty$ (**2**) were prepared by the reaction of appropriate lanthanide(III) salts and H_2PDC in DMF. Although it gave only an extremely weak data set, the isomorphous Nd^{III} compound has also been identified as containing the same major structural features as those observed in **1** and **2**. The structure of **1** is shown in Figure 1a,b.[9] Each Er^{III} cation is surrounded by seven relatively close O atoms, one from a single pendant-coordinated DMF molecule at 2.341(5) Å and six from six separate carboxylate anions at 2.275(5)−2.350(5) Å, together with a more remote O donor [2.847(5) Å] from a carboxylate anion. This gives an overall distorted square-antiprismatic geometry at the metal center.

Thermogravimetric analyses (TGA) of **1** and **2** at ambient pressure reveal two main weight losses between 20 and 400 °C before the compounds decompose at ca. 470 °C. These correspond to (i) the loss of free solvent from the channels ($T \leq 90$ °C) and (ii) the loss of coordinated DMF molecules ($T \leq 200$ °C). Following the TGA results, bulk crystalline samples of **1** and **2** were thermally treated on an IGA instrument at 85 °C under vacuum to remove all solvent molecules to form **3** and **4**, respectively, in quantitative yield.[9] Remarkably, for a lanthanide system, the sample retained its crystalline state throughout the sorption measurements.

The structure of compound **3** is shown in Figure 1c,d.[9] During removal of the coordinated DMF molecules, the bond between Er^{III} and O1N from the coordinated DMF ligand in **1** is broken. Concomitantly, two new Er−O bonds are generated by O1 and O4 changing their bridging mode from that shown in Figure 2a to that shown in Figure 2b. Thus, whereas in **1** each Er^{III} is surrounded by seven O atoms from six separate carboxylate groups (one μ_2-O and five monodentate O atoms) and a single DMF oxygen (Figure 2c), in **3** each Er^{III} is surrounded by nine O atoms from six separate carboxylate groups (three μ_2-O and three monodentate O atoms; Figure 2d). In **3**, all carboxylate anions adopt the same bridging mode (Figure 2b,d), leading to Er^{III}−carboxylate chains along the *c* axis. The PDC^{2-} anions thus bridge Er^{III} centers to form hexagonal channels, while, significantly, the pyridine N-centers remain unbound and point into the channels; these then represent potential H-bond acceptor groups.

The overall structural relationship between **1** and **3** can be visualized by considering the pseudohexagonal symmetry of **1**: applying the transformation matrix (0, $^1/_2$, $^1/_2$; 0, $-^1/_2$, $^1/_2$; 1, 0, 0) to the orthorhombic unit cell gives a pseudohexagonal cell with $a = 16.02$ Å, $c = 8.44$ Å, and $V = 1869$ Å^3. This can be compared to the hexagonal unit cell for **3** having $a = 16.22$ Å, $c = 7.41$ Å, and $V = 1690$ Å^3. Thus, the zigzag chains in **1** are observed to shorten and convert to linear chains in **3** as a result of the reorganization of the coordination sphere at the metal center following DMF removal (Figure 3).

To confirm the removal of coordinated DMF from thermally treated bulk samples, solid-state ^{13}C CPMAS NMR spectra were recorded for a fully solvated sample and for the same sample after gas storage experiments. As well as signals for the C atoms of bound PDC^{2-}, the spectrum for fully solvated **1** or **2** exhibited strong signals at 32.5 and 38.2 ppm ($-CH_3$) and at 165.9 ppm ($-CO$) assigned to DMF. No such signals were observed for the sample after heating and gas storage experiments.

Acceptable matches were observed between the experimental powder X-ray diffraction patterns (Figure 4) and those

---

(7) Hanson, K.; Calin, N.; Bugaris, D.; Scancela, M.; Sevov, S. C. *J. Am. Chem. Soc.* **2004**, *126*, 10502−10503. Dinca, M.; Long, J. R. *J. Am. Chem. Soc.* **2005**, *127*, 9376−9377. Takaoka, K.; Kawano, M.; Tominaga, M.; Fujita, M. *Angew. Chem., Int. Ed.* **2005**, *44*, 2151−2154. Chen, C.-L.; Goforth, A. M.; Smith, M. D.; Su, C.-Y.; zur Loye, H.-C. *Angew. Chem., Int. Ed.* **2005**, *44*, 6673−6677. See also: Arahams, B. F.; Jackson, P. A.; Robson, R. *Angew. Chem., Int. Ed.* **1998**, *37*, 2656−2659. Biradha, K.; Fujita, M. *Angew. Chem., Int. Ed.* **2002**, *41*, 3392−3395. Suh, M. P.; Ko, J. W.; Choi, H. J. *J. Am. Chem. Soc.* **2002**, *124*, 10976−10977.

(8) For solvent removal from lanthanide frameworks, see: Reineke, T. M.; Eddaoudi, M.; Fehr, M.; Kelley, D.; Yaghi, O. M. *J. Am. Chem. Soc.* **1999**, *121*, 1651−1657. Pan, L.; Huang, X.; Li, J.; Wu, Y.; Zheng, N. *Angew. Chem., Int. Ed.* **2000**, *39*, 527−530. Cao, R.; Sun, D.; Liang, Y.; Hong, M.; Tatsumi, K.; Shi, Q. *Inorg. Chem.* **2002**, *41*, 2087−2094. Pan, L.; Adams, K. M.; Hernandez, H. E.; Wang, X.; Zheng, C.; Hattori, Y.; Kaneko, K. *J. Am. Chem. Soc.* **2003**, *125*, 3062−3067.

(9) Crystallographic data: $C_{27}H_{23}Er_2N_5O_{14}\cdot 7.5H_2O$ (**1**), $M = 1111.13$, $a = 8.438(3)$ Å, $b = 27.795(10)$ Å, $c = 15.934(6)$ Å, $V = 3737(4)$ Å^3, $Z = 4$, orthorhombic, space group *Pnma*, $T = 150(2)$ K, $\lambda = 0.710\ 73$ Å, $D_{calcd} = 1.971$ g·cm^{-3}, $\mu = 4.53$ mm^{-1}, $R_1 = 0.041$, $wR_2 = 0.104$, $S = 1.07$; $C_{27}H_{23}N_5O_{14}Y_2\cdot H_2O$ (**2**), $M = 837.34$, $a = 8.5083(14)$ Å, $b = 28.452(5)$ Å, $c = 15.704(3)$ Å, $V = 3801.6(12)$ Å^3, $Z = 4$, orthorhombic, space group *Pnma*, $T = 150(2)$ K, $\lambda = 0.6886$ Å, $D_{calcd} = 1.463$ g·cm^{-3}, $\mu = 3.11$ mm^{-1}, $R_1 = 0.054$, $wR_2 = 0.145$, $S = 0.87$; $C_{21}H_9Er_2N_3O_{12}\cdot 3H_2O$ (**3**), $M = 883.88$, $a = b = 16.224(5)$ Å, $c = 7.412(2)$ Å, $V = 1690(1)$ Å^3, $Z = 2$, hexagonal, space group $P6_3cm$, $T = 150(2)$ K, $\lambda = 0.710\ 73$ Å, $D_{calcd} = 1.737$ g·cm^{-3}, $\mu = 5.00$ mm^{-1}, $R_1 = 0.055$, $wR_2 = 0.142$, $S = 1.07$; $C_{21}H_9N_3O_{12}Y_2\cdot 1.4H_2O$ (**4**), $M = 698.35$, $a = b = 16.239(11)$ Å, $c = 7.458(5)$ Å, $V = 1703(3)$ Å^3, $Z = 2$, hexagonal, space group $P6_3cm$, $T = 150(2)$ K, $\lambda = 0.710\ 73$ Å, $D_{calcd} = 1.362$ g·cm^{-3}, $\mu = 3.45$ mm^{-1}, $R_1 = 0.078$, $wR_2 = 0.233$, $S = 1.09$.

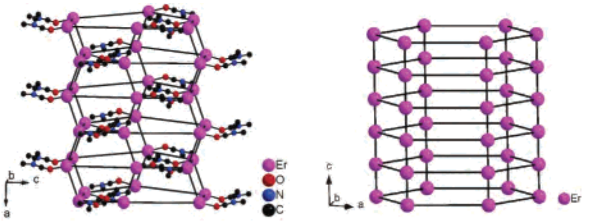

Figure 3. Schematic view of structure for **1** (left) showing coordinated DMF molecules within channels and with all PDC^{2-} ligands omitted for clarity. Schematic view of **3** (right).

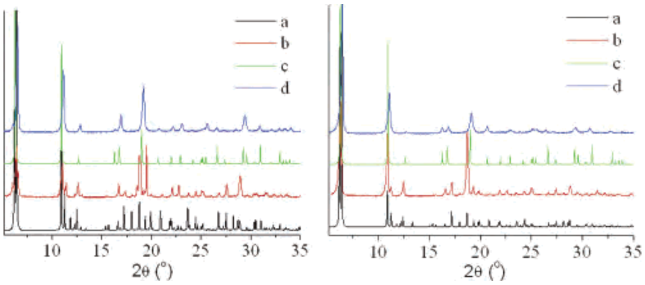

Figure 4. Powder X-ray diffraction (PXRD) patterns for compounds **1**/**3** (left) and **2**/**4** (right): (a) simulated PXRD patterns calculated from single-crystal data for the samples prior to thermal treatment; (b) experimental PXRD patterns of fresh samples of **1** and **2**; (c) simulated PXRD patterns calculated from single-crystal data for the samples after thermal treatment; (d) experimental PXRD patterns of samples of **3** and **4** after degassing.

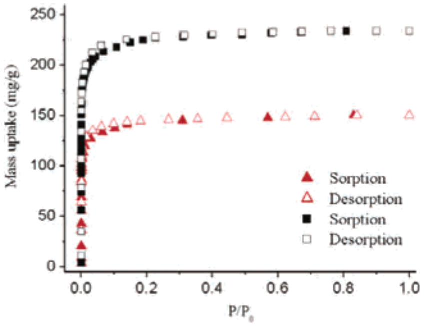

Figure 5. N_2 adsorption isotherms (77 K) for **3** (red) and **4** (black).

simulated from single-crystal X-ray data for bulk crystalline samples of solvated **1** and **2** and desolvated **3** and **4** after thermal treatment. These data confirm general structural transfer after solvent removal for bulk samples, but the presence of amorphous material cannot be discounted.

Gas storage studies were performed on samples of complexes **1**−**4**. No N_2 or H_2 uptake was observed for samples of **1** or **2**, which contain both coordinated and sorbed solvent. However, after removal of guest and coordinated solvent molecules, N_2, H_2, and benzene uptake was observed for both **3** and **4**. Significantly, therefore, heating **1** and **2** triggers loss of both sorbed and coordinated solvent coupled with rearrangement of the metal−ligand framework core to afford porous **3** and **4**, respectively.

N_2 adsorption by **3** and **4** at 77 K (Figure 5) shows reversible type I isotherms characteristic of microporous materials with uptakes of 168 (for **3**) and 235 mg·g^{-1} (for **4**) and calculated BET surface areas of 427 (for **3**) and 676 m^2·g^{-1} (for **4**). Benzene vapor adsorption by **3** and **4** at 300 K (Figure 6) also shows reversible type I isotherms indicative of effective micropore filling by benzene. H_2 adsorption was measured at 77 K (Figure 7) at pressures of up to 1 bar, and

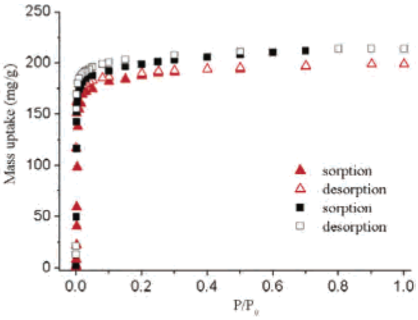

Figure 6. Benzene adsorption isotherms (300 K) for **3** (red) and **4** (black).

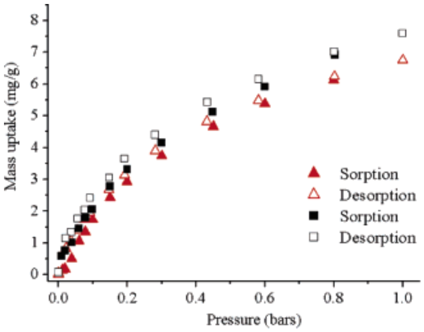

Figure 7. H_2 adsorption isotherms (77 K) for **3** (red) and **4** (black).

saturation was not achieved at this pressure. The occupancy of the channels was assessed as 8.8 N_2, 4.2 C_6H_6 (saturated amount), and 5.6 H_2 (1 bar) molecules per unit cell for **3** and 11.4 N_2, 3.7 C_6H_6 (saturated amount), and 5.1 H_2 (1 bar) molecules per unit cell for **4**. For N_2 and C_6H_6 adsorption, both **3** and **4** exhibit $q_{st,\Phi=1/e}$ values similar to those of activated C: for N_2, 13.44 kJ·mol^{-1} for **3**, 13.05 kJ·mol^{-1} for **4**, and ∼12 kJ·mol^{-1} for activated C;[10] for C_6H_6, 57.39 kJ·mol^{-1} for **3**, 62.20 kJ·mol^{-1} for **4**, and ∼60 kJ·mol^{-1} for activated C.[11]

In summary, we have successfully constructed a robust, open, metal−organic framework from lanthanide metal cations and PDC^{2-} anions, obtaining the bulk materials readily in a one-pot reaction. Upon removal of the bound DMF molecules, a porous framework is thus generated from a previously non-porous material. This structural transfer is the first crystallographically characterized system with lanthanide metal ions.

Acknowledgment. We thank EPSRC for support and CVCP and University of Nottingham for funding (to J.J.). We are grateful to CCLRC for access to Stations 9.8 and 16.2smx on the Daresbury SRS and to Drs. J. E. Warren and T. J. Prior for experimental advice. We also acknowledge Dr. J. J. Titman for assistance with solid-state ^{13}C NMR measurements. M.S. gratefully acknowledges receipt of a Royal Society Wolfson Merit Award and of a Royal Society Leverhulme Trust Senior Research Fellowship.

Supporting Information Available: Synthetic procedures, characterization, X-ray data and details (CIF), sorption isotherms, and parameters. This material is available free of charge via the Internet at http://pubs.acs.org.

IC061095U

---

(10) Kaneko, K. *Langmuir* **1987**, *3*, 357−363.

(11) Ramirez, D.; Qi, S.; Rood, M. *Environ. Sci. Technol.* **2005**, *39*, 5864−5871.